

UNCLASSIFIED

Defense Technical Information Center  
Compilation Part Notice

ADP012552

TITLE: Analytic Potentials for Realistic Electrodes

DISTRIBUTION: Approved for public release, distribution unlimited

This paper is part of the following report:

TITLE: Non-Neutral Plasma Physics 4. Workshop on Non-Neutral Plasmas  
[2001] Held in San Diego, California on 30 July-2 August 2001

To order the complete compilation report, use: ADA404831

The component part is provided here to allow users access to individually authored sections of proceedings, annals, symposia, etc. However, the component should be considered within the context of the overall compilation report and not as a stand-alone technical report.

The following component part numbers comprise the compilation report:

ADP012489 thru ADP012577

UNCLASSIFIED

# Analytic Potentials for Realistic Electrodes

S. E. Barlow, A.E. Taylor and K. Swanson

*W.R. Wiley Environmental Molecular Sciences Lab  
Pacific Northwest National Laboratory  
P.O. Box 999 (K8-88)  
Richland, WA 99352*

**Abstract.** We show how LaPlace's equation can be accurately solved when the boundary conditions are not amenable to direct analytic treatment. This problem arises for nearly all real electrodes. Our approach systematically combines numerical relaxation techniques with analytic expansions to produce a provably unique solution.

## INTRODUCTION

Many problems in physics and engineering begin with a solution to LaPlace's equation:

$$\nabla^2 \Phi(\mathbf{r}) = 0 \quad (1)$$

where  $\Phi(\mathbf{r})$  is a potential in some volume of space determined by the boundary conditions. Analytic solutions to this partial differential equation are limited to geometries that precisely match an orthogonal coordinate system. For example, eq. (1) can be readily solved for the rectangular or cylindrical box by the method of separation of variables. Although this method is very powerful, by itself it suffers from at least two shortcomings. First, the solutions take the form of infinite sums over special functions and are rather difficult to interpret physically. And second, the rigorous requirements of the boundaries are almost never met in practise. For instance, in electrostatic problems, gaps between electrodes are required to maintain potential differences, further in real instruments it is often necessary to put holes in the electrodes to provide access to the internal volume. Sometimes it is desirable to shape boundary electrodes that do not even approximately match those of an orthogonal coordinate system, e.g., the hyperbolic ion trap. Finally, the analytical techniques cannot readily account for construction errors that inevitably arise in real devices.

Equation (1) may also be solved numerically. In recent years, computer codes have been developed to tackle some of the short comings listed above. In these codes, the boundary conditions are mapped onto a grid. The potential is then found by a series of "relaxation" calculations. The most widely used of these codes is the SIMION[1], but others are available. These codes produce a "potential array" for

the volume of interest. Like the analytical approaches mentioned above, numerical solutions tend to provide little direct insight into the physics of interest.

A powerful technique for providing insight into the physical consequences of a potential is the "multipole-pole" expansion. The multipole expansion of a potential may be formally accomplished by writing the solutions to eq. (1) in spherical coordinates and then changing to the desired coordinate system—generally cylindrical polar  $(r, \theta, z)$  or cartesian  $(x, y, z)$  coordinates. For example in cylindrical-polar coordinates, with cylindrical symmetry the solution of eq. (1) is

$$\Phi(r, z) = V \sum_{n=0}^{\infty} \frac{C_n}{r_0^n} \Phi_n(r, z) \quad (2)$$

where  $V$  is some potential value;  $r_0$  is a distance or size scaling factor; the  $C_n$  are the constants to be determined from the boundary conditions; and  $\Phi_n(r, z)$  are the various "orders" of the solution to eq. (1). Since many electrostatic problems have cylindrical symmetry, and the treatment is simpler (two instead of three dimensions) all further discussions here will be limited to this case. The multipole expansion is particularly useful because the behavior of a system is normally governed by the lowest order terms that are present in the potential. The trick is to find a way to reliably and accurately evaluate the  $C_n$ 's. In the following section, we outline the steps that allow us to evaluate these constants from numerical calculations. (Much more detail is provided in our paper, scheduled for publication in 2001.[2])

## EVALUATION OF MULTIPOLE COEFFICIENTS FROM NUMERICAL RELAXATION CALCULATIONS

Computation of the  $C_n$ 's proceeds in four steps. First, the boundary value problems is set-up using some sort of numerical relaxation calculation. Second, we extract from the relaxation calculation the potential over a "virtual Gaussian surface." In the third step, this virtual surface is used to evaluate the coefficients in the sums of the formal solution of eq. (1). Finally, the formal solution is expanded term by term in a Taylor series to evaluate the  $C_n$ 's.

### Setting up the Problem

In general the problem is set up by defining the symmetries, boundary shapes and grid size through the GUI of the relaxation code, e.g. SIMION. Care must be taken to insure that the grid is sufficiently fine to resolve the details of the problem adequately. SIMION uses a uniform cartesian grid, which simplifies the next step, but the cost is some loss of precision. While we have no requirement for a uniform mesh (grid) we do need to have the potential specified on cylindrical surfaces

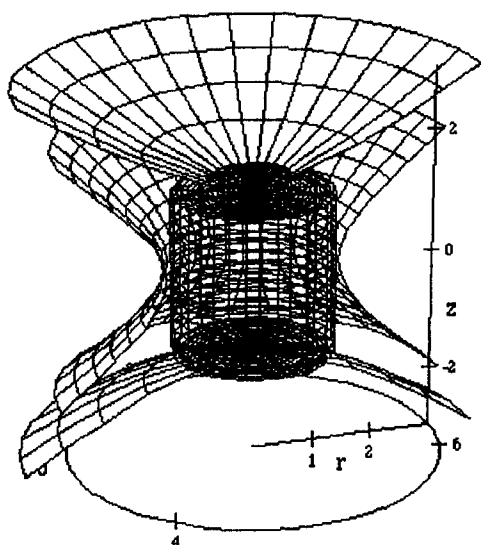


**FIGURE 1.** Schematic of hyperbolic trap electrodes and inscribed cylinder.

$(r = a, z)$  and  $(r, z = z_{\text{bottom or top}})$  where  $a$  is the radius and  $z_{\text{bottom or top}}$  are the end of our “virtual Gaussian” surface.

### Extracting the “Virtual Gaussian Surface”

As a practical matter, the bulk of the real work is done when the relaxation calculation has been performed. However, we are left with an array of numbers—the potential array—that may have  $10^6$  or more elements. What we must do next is to define our inscribed cylindrical surface such that it is as large as possible, but does not include any conductors. The cylinder’s axis of symmetry needs to coincide with the symmetry axis of the problem. We also need to define a  $z = 0$  plane and “top” and “bottom” planes. This cylinder’s dimensions must be chosen to exactly match a line of grid points. With the cylinder so defined, we can then select those points in the potential array that fall on the cylinder’s surface. The SIMION code does not give direct access to the potential array file. We have written a small program that allows us to extract those portions of this file that we need for the calculations of the next section. This program and some documentation is available on the world wide web.[3]

## The Analytic Potential

The solution of eq. (1) in a cylindrically symmetric domain that includes the axis of symmetry is

$$\Phi(r, \theta, z) = \sum_{s=0}^{\infty} \left\{ \alpha_{1,s} \cos \left[ \frac{(2s+1)\pi(2z-z_t-z_b)}{2(z_t-z_b)} \right] I_0 \left[ \frac{(2s+1)\pi r}{2(z_t-z_b)} \right] + \alpha_{2,s} \sin \left[ \frac{2s\pi(2z-z_t-z_b)}{2(z_t-z_b)} \right] I_0 \left[ \frac{4s\pi r}{2(z_t-z_b)} \right] \right\} + \sum_{s=1}^{\infty} \left\{ \alpha_{3,s} \sinh \left[ \frac{(z-z_t)j_s}{c} \right] J_0 \left[ \frac{j_s r}{c} \right] - \alpha_{4,s} \sinh \left[ \frac{(z-z_b)j_s}{c} \right] J_0 \left[ \frac{j_s r}{c} \right] \right\} \quad (3)$$

Here,  $J_0(x)$  is the Bessel function of the first kind of order 0; and  $I_0(x)$  is the modified Bessel function of order zero. The symbol  $j_s$  is the  $s^{\text{th}}$  zero of  $J_0(x)$ . If we designate the potential on the top of the cylinder as  $V_t(r, z = z_t)$ , that on the bottom as  $V_b(r, z = z_b)$  and on the side as  $V_r(r = c, z)$  we find for the  $\alpha$ 's:

$$\alpha_{1,s} = \frac{2}{(z_t - z_b) I_0 \left[ \frac{(2s+1)\pi c}{2(z_t - z_b)} \right]} \int_{z_b}^{z_t} V_r(z) \cos \left[ \frac{(2s+1)\pi(2z - z_b - z_t)}{2(z_t - z_b)} \right] dz, \quad (4)$$

$$\alpha_{2,s} = \frac{2}{(z_t - z_b) I_0 \left[ \frac{4s\pi c}{2(z_t - z_b)} \right]} \int_{z_b}^{z_t} V_r(z) \sin \left[ \frac{2s\pi[2z - z_b - z_t]}{z_t - z_b} \right] dz, \quad (5)$$

$$\alpha_{3,s} = \frac{2}{c^2 \sinh \left( \frac{(z_t - z_b)j_s}{c} \right) [J_1(j_s)]^2} \int_0^c V_b(r) J_0 \left( \frac{j_s r}{c} \right) r dr \quad (6)$$

and

$$\alpha_{4,s} = \frac{2}{c^2 \sinh \left( \frac{(z_t - z_b)j_s}{c} \right) [J_1(j_s)]^2} \int_0^c V_t(r) J_0 \left( \frac{j_s r}{c} \right) r dr. \quad (7)$$

where we use  $V(r, z)$  found from the finite difference calculations as described below. The  $\alpha$ 's tend to become rapidly small with  $s$ , so we find that only a few of these terms need to be explicitly evaluated unless we are interested in the solution very near a boundary. If the  $(x, y)$  plane at  $z = 0$  is also a symmetry plane, the eqs (3) to (7) simplify because  $\alpha_{2,s} = 0$  and  $\alpha_{3,s} = -\alpha_{4,s}$ .

## The Multipole Expansion

Having found the  $\alpha$ 's, the multipole expansion can be accomplished easily. We set  $r = 0$  in eq.(3), since  $J_0(0) = I_0(0) = 1$ , we are left with trigonometric and hyperbolic trig functions whose power law expansions in  $z$  are readily found. Since each power of  $z$  is linearly independent, we merely collect like terms and add them up. By eq.(2), the sums for some power of  $z$ , say  $n$  is simply  $C_n/r_0^n$ .

The values we find for  $C_n$  are correct to within the accuracy of our initial relaxation calculation. They are also complete and unique, with respect to our choice of  $z = 0$ . Sometimes the choice of the origin will not be immediately obvious,

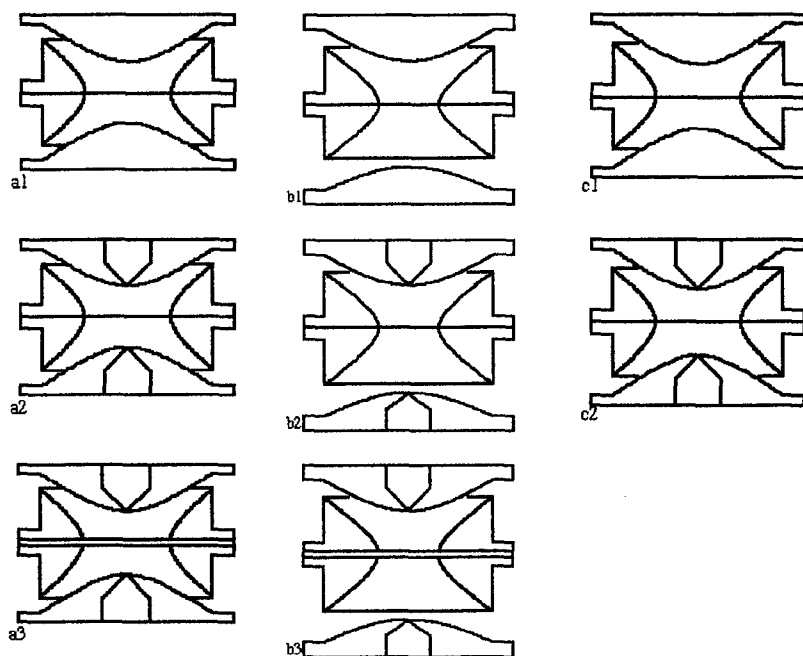


**FIGURE 2.** Sketches of various electrodes for which calculations were performed, see text and tables.

techniques for finding the point are discussed by Barlow et al.,[2] but lie outside the scope of this summary.

**TABLE 1.** Calculated even order  $C$ 's for nine variants of hyperbolic electrode structures

| Trap Type       | Fig. 2. | $C_0$  | $C_2$   | $C_4$            | $C_6$            |
|-----------------|---------|--------|---------|------------------|------------------|
| "Ideal" Trap    |         | 0.5    | -1      | 0                | 0                |
| Truncated Trap  | a1      | 0.5007 | -0.9799 | $1.23(10)^{-4}$  | $1.07(10)^{-3}$  |
| + endcap holes  | a2      | 0.5010 | -0.9784 | $4.52(10)^{-3}$  | $1.26(10)^{-2}$  |
| + ring slot     | a3      | 0.4838 | -1.0044 | $-2.72(10)^{-2}$ | $5.77(10)^{-2}$  |
| Stretched Trap  | c1      | 0.5567 | -0.8777 | $-1.51(10)^{-2}$ | $-6.40(10)^{-3}$ |
| + endcap holes  | c2      | 0.5569 | -0.8767 | $-1.26(10)^{-2}$ | $-1.02(10)^{-3}$ |
| Asymmetric Trap | b1      | 0.5007 | -0.9801 | $-2.26(10)^{-4}$ | $8.02(10)^{-4}$  |
| + endcap holes  | b2      | 0.5009 | -0.9792 | $2.13(10)^{-3}$  | $6.72(10)^{-3}$  |
| + ring slot     | b3      | 0.4818 | -0.9855 | $-3.07(10)^{-2}$ | $4.61(10)^{-2}$  |

**TABLE 2.** Calculated odd order C's for nine variants of the hyperbolic electrode structure. Numbers in parenthesis are nominally zero. The \* denotes value that were set to zero.

| Trap Type       | Fig. 2. | C <sub>1</sub>  | C <sub>3</sub>   | C <sub>5</sub>   |
|-----------------|---------|-----------------|------------------|------------------|
| "Ideal" Trap    |         | 0               | 0                | 0                |
| Truncated Trap  | a1      | $-1.[10]^{-9}$  | $3[10]^{-9}$     | $3[10]^{-9}$     |
| + endcap holes  | a2      | $-9.[10]^{-10}$ | $3[10]^{-9}$     | $-2[10]^{-9}$    |
| + ring slot     | a3      | $-2[10]^{-9}$   | $6[10]^{-9}$     | $-5[10]^{-9}$    |
| Stretched Trap  | c1      | $-1[10]^{-9}$   | $3[10]^{-9}$     | $-2[10]^{-9}$    |
| + endcap holes  | c2      | $-1[10]^{-9}$   | $2[10]^{-9}$     | $-1[10]^{-9}$    |
| Asymmetric Trap | b1      | 0*              | $-3.06(10)^{-4}$ | $-3.30(10)^{-4}$ |
| + endcap holes  | b2      | 0*              | $-1.45(10)^{-3}$ | $-3.81(10)^{-3}$ |
| + ring slot     | b3      | 0*              | $-5.18(10)^{-3}$ | $-6.55(10)^{-3}$ |

## DISCUSSION

Figure (2) illustrates eight variations of hyperbolic electrodes for which we have done calculations. In each case, the hyperbolae were truncated at  $2.8r_0$  to closely match electrode structures that we possess in the laboratory. The trap geometries labeled a1,a2, and a3, are symmetric trap structures with the endcap spacing  $2z_0 = 2\sqrt{2}r_0$ , where we successively add end cap holes and a ring slot to the already truncated and flanged electrodes. The end cap holes were set at  $0.075r_0$  and the ring slot at closely match actual trap electrode structures. The structures labeled b1, b2, and b3 are asymmetric trap structures[4], with similar endcap holes and ring slot. The two structures labeled c1 and c2 have electrode shapes that are identical to those of a1 and a2, but the endcap spacing has been increased by 10.8% as is standard commercial practice.

Table 1 summarizes the even order coefficients for each of these trap geometries, while Table 2 shows our evaluation of the odd order.

## REFERENCES

1. D.A. Dahl, SIMION 3D, V6.0, INEEL, Idaho Falls, ID, 1995.
2. S.E. Barlow, A.E. Taylor and K. Swanson, *Int. J. Mass Spectrom.*, **207**, pg. 19, 2001.
3. Potential Extraction program is available at:  
<http://www.emsl.pnl.gov/docs/idl/software/SimionPAViewer.html>.
4. M.L. Alexander, S.E. Barlow and J. Follansbee, *Proc. 46th ASMS Conf.*, pg. 1173 1998.
5. J. Franzen, R.H. Gabling, M. Schubert and Y. Wang, in: *Practical Aspects of Ion Trap Mass Spectrometry*, Vol. 1, R.E. March and J.F.J. Todd, eds., CRC Press, NY (1995) Ch. 3.